

Pulse propagation in optical fibers near the zero dispersion point

M. Klauder, E. W. Laedke, K. H. Spatschek, and S. K. Turitsyn
*Institut für Theoretische Physik I, Heinrich-Heine-Universität Düsseldorf,
 D-4000 Düsseldorf 1, Germany*

(Received 10 February 1993)

The problem of nonlinear pulse propagation in optical fibers near the zero dispersion point is investigated. It is shown, both analytically and numerically, that stable double-humped solitary-wave solutions potentially can be used for transmission. The results clarify previous problems with the existence of single-humped localized solitary waves, i.e., fundamental solitons, which are forbidden in the strict mathematical sense.

PACS number(s): 42.81.Dp, 42.65.Re

Since the pioneering theoretical [1] and experimental [2] works on the problem of soliton propagation in optical fibers the field has grown significantly. It is now a common belief that solitons are important in fiber optics. Typical examples for applications are long-distance optical communication systems and optical switching devices (see, for example, the review [3]). Solitons also are important for the modeling of the different types of mode-locked ring lasers [4,5].

The peak pulse power necessary to establish a fundamental bright soliton in fibers is inversely proportional to the square of the pulse duration and directly proportional to the fiber dispersion. Therefore, a natural way to reduce the power required for launching a pulse with fixed duration is to use a wavelength where the dispersion is minimal. The linear dispersion results from both the material of the fiber and the geometrical characteristics of the fiber. At the so-called zero-dispersion point (ZDP) the second-order dispersion vanishes and the total fiber dispersion is minimal. The power required to generate a bright soliton near the ZDP is consequently much smaller than that required in the region of anomalous dispersion; but it is known that pulses launched very close to or exactly at the ZDP cannot propagate for a long time at this wavelength, because of the self-phase-modulation (SPM)-induced spectral broadening. As a consequence of the resulting time-dependent nonlinear phase shift, the pulse creates its own second-order dispersion (see, e.g., Refs. [6,7]). The value of such an induced second-order dispersion may be estimated by the relation $k'' \approx k''' |\delta\omega_{\max}| / 2\pi$. Here $\delta\omega_{\max}$ is a maximum of the SPM-induced spectral broadening, which depends on the initial parameters of the pulse, and is larger for pulses with higher peak powers. The prime denotes the derivative of the wave number k with respect to the frequency ω .

As has been demonstrated in [7,8], for a given pulse width the minimum power required to establish a soliton-type pulse near the ZDP is really substantially lower than the power required to launch a soliton in the anomalous dispersion region. It was also discovered that the wave packet forming near the ZDP has a solitonlike form that radiates continuously [10]. The amplitude of radiation is small when the frequency shift from the ZDP is large enough [11]. In this Rapid Communication we demonstrate that the main reason for the appearance of radiation is the absence of symmetry for the one-hump

fundamental soliton. We find that bound states in the form of two coupled fundamental solitons possess the appropriate symmetry; they do not emit radiation. We will present simple analytical descriptions of these solutions that are in good agreement with the numerics. We also demonstrate numerically that bound states with well-separated humps are quite stable against small perturbations, so that they can be used, in a certain parameter regime, for transmission.

SPM and group-velocity dispersion, which are important for soliton propagation in fibers, also play an important role in the problems of the *generation* of nonlinear pulses (see, e.g., [4]). As was noted [5], there is a certain wavelength that separates the stable and unstable regimes of the operation of colliding-pulse mode-locked (CPM) rings lasers. This wavelength is critical from the point of view of dispersion, and may be considered as a generalized ZDP, which is appropriate to the dye laser. This analogy was recently confirmed experimentally [5]. Thus we believe that our results may be applicable not only to the problem of the nonlinear pulses' propagation in fibers near the ZDP, but also to other problems where higher-order dispersion plays a significant role.

Let us start with the structure of pulses in single-mode fibers near the ZDP. The pulse envelope propagation in optical fibers near the ZDP is governed by a modified nonlinear Schrödinger equation (NSE) [9–13]

$$i(E_z + k'E_t) - \frac{k''}{2}E_{tt} - \frac{i}{6}k'''E_{ttt} + k\frac{n_2}{n_0}\rho|E|^2E = 0, \quad (1)$$

where n_2 is the Kerr coefficient, k is the wave number, $k' = dk/d\omega$, n_0 is the linear part of the refractive index, and ρ is a geometrical factor. We consider a wavelength region $\Delta\lambda$ around the zero dispersion wavelength λ_0 where $|k''|\tau \geq |k'''|$ (τ is the pulse width). It is convenient to reduce Eq. (1) to a dimensionless form

$$i\psi_z + \psi_{TT} - \psi + |\psi|^2\psi = i\kappa(\psi_{TTT} - \psi_T), \quad (2)$$

by using the following transformation:

$$\psi(Z, T - \kappa Z)e^{iZ} = \left[\frac{2\tau^2\alpha}{|k''|} \right]^{1/2} E(z, t), \quad \alpha = \frac{kn_2\rho}{n_0},$$

$$T = \frac{t - k'z}{\tau}, \quad Z = \left[\frac{|k''|}{2\tau^2} \right] z,$$

where τ is a typical pulse length. For a single-mode fiber with parameters discussed, e.g., in Ref. [14], near the ZDP we have

$$\kappa = -k'''/3|k''|\tau \approx 7 \times 10^{-4} \frac{\lambda(\mu\text{m}) - 0.86}{\tau(\text{psec})[1.27 - \lambda(\mu\text{m})]}.$$

In [11] it was shown that fundamental solitons are destroyed by a third-order dispersion term, and radiation is caused by the latter. Kuehl and Zhang [15] calculated the radiation, confirming the results of Wai, Chen, and Lee [11]. The main point in these investigations is that the localized *single-humped* fundamental soliton solutions of Eq. (2) for $\partial_z = 0$ should fulfill the boundary condition $|\psi| \rightarrow 0$ as well as the symmetry relation $\psi(T) = \psi^*(-T)$. This means that $\text{Re}\psi$ is symmetric, while $\text{Im}\psi$ is antisymmetric with respect to T . Expanding with respect to small κ , Wai, Chen, and Lee [11] showed that for single-humped solutions

$$\text{Im}\psi_{TT}|_0 \ll \kappa^m \tag{3}$$

for all m , i.e., the antisymmetry is satisfied in an asymptotic expansion to all polynomial orders. Nevertheless, an analysis beyond all orders showed that the proper solutions do not satisfy $\text{Im}\psi_{TT}|_0 = 0$; the deviation is of the order of $\exp(-\pi/2\kappa)$. This elegant mathematical finding corresponds to the physically observed slow decay of fundamental solutions.

The new localized “stationary” solutions of Eq. (1) presented here are of a double-hump form and can be interpreted as a superposition of two coupled fundamental solitons. They do not have radiation tails for $|T| \rightarrow \infty$. It should be noted that, contrary to the two-soliton solutions of an ordinary NSE, the double-humped solitons are apparently “stationary” pulses. Similar structures were observed in experiments with a passively mode-locked neodymium fiber laser [16]. In the latter experiments it was found that the multiple pulses do not change with increasing cavity round-trip time, i.e., multiple-pulse outputs cannot be attributed to higher-order soliton solutions of a usual NSE.

We have found that localized solutions can be presented in the form $\psi = \psi_0 + \delta\psi$, where ψ_0 is a localized double-humped solution

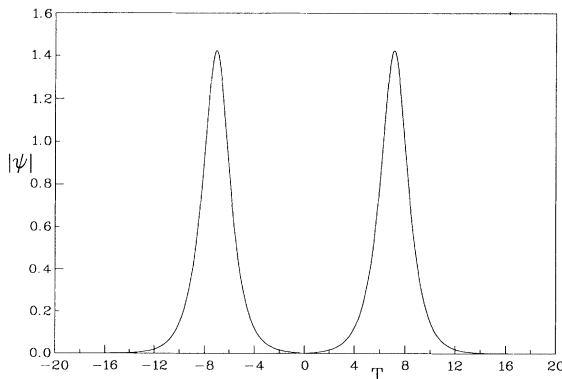


FIG. 1. A “stationary” ($\partial_z = 0$) solution of Eq. (2). The absolute value of ψ is shown vs T for $\kappa = 0.1119$. Note that the two humps are well separated. In the nonstationary problem this form is unchanged up to $Z \approx 1000$.

$$\psi_0 \equiv G(T_0 + T) + G^*(T_0 - T), \tag{4}$$

and $\delta\psi$ corresponds to trapped radiation ($\delta\psi \ll \psi_0$), decaying to zero for $|T| \rightarrow \infty$. All the solutions obey the requirement of exponential decay at infinity and fulfil the following symmetry conditions at $T = 0$:

$$\text{Im}\psi|_0 = \text{Re}\psi_T|_0 = \text{Im}\psi_{TT}|_0 = 0. \tag{5}$$

Generally, two types of solutions appear, alternating with increasing (discrete) κ values: solutions with $\text{Re}\psi|_0 = \text{Im}\psi_T|_0 = 0$ (type I) on the one hand, and $\text{Re}\psi|_0 \approx \kappa \text{Im}\psi_T|_0 \neq 0$ (type II) on the other hand.

It is straightforward to calculate G to any order in κ ; e.g., for a type-I solution we obtain

$$G(z) = \frac{\sqrt{2}}{\cosh(z)} e^{-i\alpha} \left[1 + i \frac{3}{2} \kappa \tanh(z) - \frac{39}{8} \kappa^2 + \frac{21}{4} \frac{\kappa^2}{\cosh^2(z)} - i \frac{107}{16} \kappa^3 \tanh(z) + i \frac{151}{8} \kappa^3 \frac{\tanh(z)}{\cosh^2(z)} + \dots \right]. \tag{6}$$

and $\delta\psi(z) \approx A \exp(iz/\kappa)$ for $z \rightarrow 0$. Without going into too many details, let us mention that the idea is to superimpose symmetrically two single-humped soliton solutions including their radiation tails. The functions consist of exponentially decaying tails and oscillatory parts. We match the two solutions (including the tails) for $|T| \ll T_0$, and thereby get discrete eigenvalues κ for the existence of completely localized double-humped eigenstates. In Fig. 1 a typical solution is shown.

The continuity of (the two parts of) ψ and ψ_T at $T = 0$ determines the phase α , e.g.,

$$\alpha \approx \frac{\pi}{2} + \frac{\kappa}{2} \tag{7}$$

up the first order in κ . The two humps of the solutions are more separated the smaller κ is. The dependence of T_0 on κ is shown in Fig. 2. Note that the relevant κ values are discrete, but a continuum approximation becomes valid for $\kappa \rightarrow 0$. Within the latter, a simple model calculation leads to the following evolution equation for

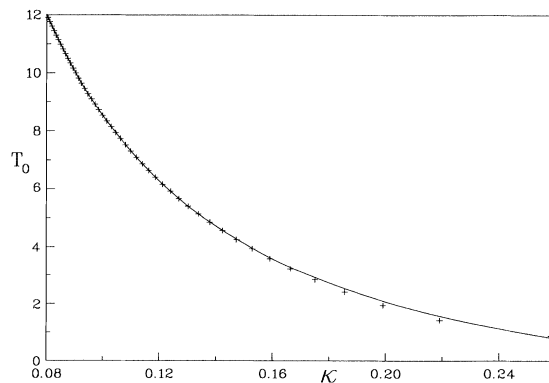


FIG. 2. Hump position T_0 vs κ . The crosses designate the discrete eigenvalues found from numerics. The solid line is our analytical result (9), being valid in the continuum approximation.

the average distance between the two peaks (e.g., for type-I solutions):

$$\begin{aligned} \frac{\partial^2}{\partial Z^2} \int_0^\infty T |\psi|^2 dT \\ \approx 3 \times 2^5 e^{-2T_0} \sin^2(\alpha) \\ + \frac{3 \times 2^5 C}{\kappa^2} e^{-T_0} \sin(\alpha) e^{-\pi/2\kappa} \sin\left[\frac{T_0}{\kappa} - \alpha\right]. \end{aligned} \quad (8)$$

The derivation of this relation starts from Eq. (2). After appropriate manipulations we use the symmetry relations (5) and calculate some coefficients by using the approximate form (6); C is a numerical constant which can be determined from some well-defined integrals. It should be noted that the constant C can be calculated analytically. However, one will find that many terms in the expansion (6) contribute to the value of C ; the convergence with higher orders in κ is very slow. In order to avoid unessential complexity here, we evaluate C numerically; $C \approx 12.94$. Equating the right-hand side of Eq. (8) to zero for stationary solutions we obtain (for both type-I and type-II solutions)

$$T_0 \approx \frac{\pi}{2\kappa} + 2 \ln \kappa - \ln C. \quad (9)$$

This is a very useful relation between the eigenvalues κ and the distance ($2T_0$) between the two humps of the “stationary” solution (see Fig. 1).

The matching of the oscillatory parts at $T=0$ gives the relation $(T_0/\kappa) - \alpha \approx n\pi$, where n is an integer. From this additional condition we can determine the spacing between the discrete eigenvalues $\kappa = \kappa_n$. Defining $\kappa_{n+1} = \kappa_n + \delta\kappa_n$, and making use of Eq. (9), a short calculation leads to

$$\delta\kappa_n \approx \frac{-\kappa_n^3}{1 - \frac{2}{\pi} \kappa_n \left[1 - \ln \kappa_n + \frac{\ln C}{2} \right] + \frac{\kappa_n^3}{2\pi}}, \quad (10)$$

for both the type-I and type-II solutions. We should mention that the three relations presented in Eqs. (7), (9), and (10), respectively, agree excellently with the numerical findings. For example, in Fig. 2 the solid line shows

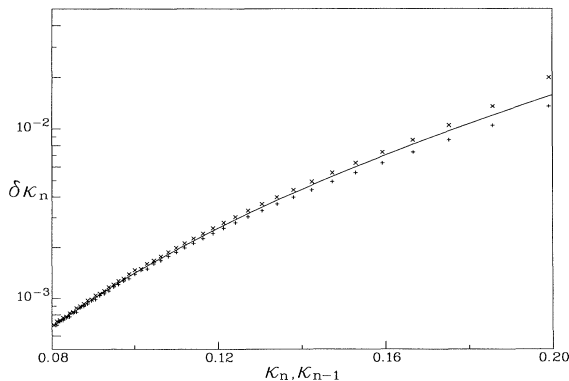


FIG. 3. Eigenvalue spacings $\delta\kappa_n = \kappa_{n+1} - \kappa_n$ (logarithmic scale) vs κ_n (denoted by \times) and κ_{n-1} (depicted by $+$) (both in logarithmic scales), respectively. The solid line represents the analytically found relation (10).

the curve (9) (for $\ln C \approx 2.56$). It is a very good fit to the numerically found discrete $\kappa - T_0$ relation (shown by crosses). In Fig. 3 we depict the eigenvalue spacings $\delta\kappa_n$ versus κ_n (denoted by \times) and κ_{n-1} (depicted by $+$). The solid line represents the relation (10). Again the agreement is excellent. We have also investigated the fine structures of the “stationary” solutions and examined in detail the matching via radiation tails. Details will be published elsewhere. As a result we can state that higher-order dispersion leads to the pinning of fundamental solitons in the form of double-humped localized solutions. This phenomenon is presumably quite general for higher-order dispersion [17] and may be found also in other problems with higher-order dispersive effects. It should be also mentioned that we expect that a whole family of multiple-humped solutions will exist.

Next, we investigate the stability of the newly found solutions. The general result is that, for small κ , corresponding to large distances $2T_0$ between the humps, the solutions are stable over long propagation distances, whereas for large κ values the solutions are quite rapidly destroyed. A typical example for an unstable solution is shown in Fig. 4 for $\kappa \approx 0.22$. The solution is completely destroyed after $Z \approx 120$ if we start at $Z=0$ with an exact stationary double-hump pulse ($T_0 \leq 2$). On the other hand, and this is physically most important, for $\kappa \leq 0.11$ ($T_0 \geq 7$) the solutions are very stable over long distances ($Z > 10^3$). To appreciate these findings, we have to take into account

$$\kappa \approx \frac{2.87 \times 10^{-4}}{\tau(\text{psec}) \Delta\lambda(\mu\text{m})}, \quad z(\text{km}) \approx \frac{6\kappa[\tau(\text{psec})]^3}{|k''''| \left[\frac{\text{psec}^3}{\text{km}} \right]} Z, \quad (11)$$

leading to $z(\text{km}) \approx 1.4 Z$ for $\tau = 0.57$ psec, $\Delta\lambda \approx 5 \times 10^{-3}$ μm , $|k''''| = 0.08$ psec³/km, i.e., $\kappa \approx 0.1$. Thus, if the pulses are well separated, they can move without significant changes in shapes over distances of several thousands of kilometers. A typical example is the solution ($\kappa = 0.1119$) shown in Fig. 1. When inserted into the Z -dependent equation as initial distribution, we do not observe any significant changes in shape up to $Z \approx 10^3$,

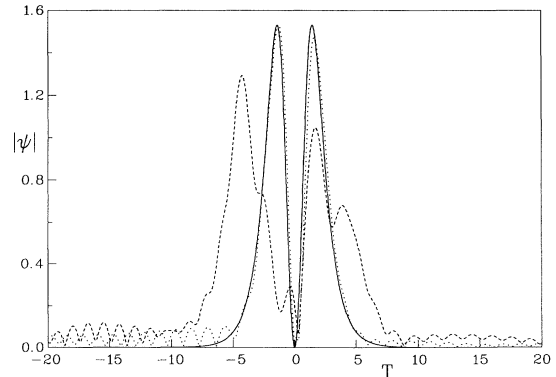


FIG. 4. Z dependence of a “stationary” ψ solution under perturbations, for $\kappa = 0.22$. The absolute value $|\psi|$ as a function of T is shown for $Z=0$ (solid line), 110 (dotted line), and 120 (broken line), respectively. In contrast to the results for small κ values (see, e.g., Fig. 1), the solution is unstable and rapidly destroyed.

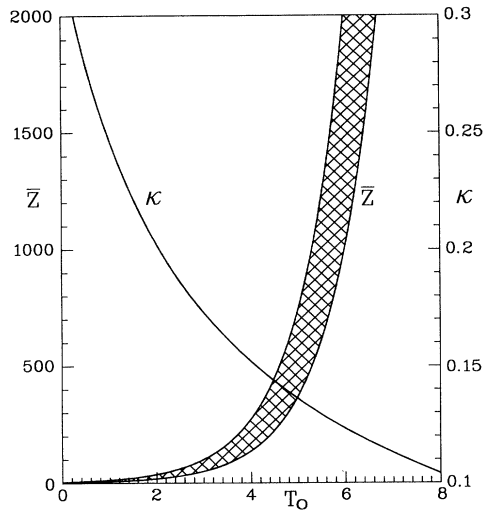


FIG. 5. Scaling of the "life distances" \bar{Z} (left ordinate) of double-humped solutions as a function of the humps' separation T_0 . The width of the curve originates from numerics. On a different scale (right ordinate) we have plotted $\kappa = \kappa(T_0)$, so that it is easy to estimate the life distance for a given κ .

even if noise is added initially. (This is the reason why we do not present additional figures for nonvanishing Z values for that κ value. In that parameter regime, changes would not be observable.) This behavior, of course, stimulates the question: How do the characteristic decay times of the bound states scale with κ ? Defining $\bar{Z}^{-1} = |\partial \ln \psi / \partial Z|$ we find from our simple and intuitive analytical approach (8)

$$\bar{Z} \approx e^{T_0}, \quad (12)$$

where for $T_0 = T_0(k)$ we can use the expression (9). This scaling clearly explains why for $\kappa \leq 0.11$ no significant changes are observed at distances $Z \approx 10^3$, which are of practical importance. In Fig. 5 we demonstrate this theoretical prediction (12). The scaling (12) is confirmed by plotting the approximate life distances \bar{Z} as a function

of T_0 from the numerical simulations. Note that $\bar{Z} \sim \exp(T_0)$ holds for small κ , although there is some uncertainty in defining \bar{Z} directly (e.g., from the inverse growth rates of the pulse separation).

Finally, let us mention another aspect that is also of great practical importance. When generating the pulses we cannot expect to tailor exactly the forms of the "stationary" (and quite stable) solutions considered here. From the mathematical point of view, since Eq. (1) is not completely integrable, there is no evidence that any initial distribution will finally evolve into the pulses (4); however, our numerical simulations showed that the stable propagation of two-humped pulses is a rather general case of evolution. When prescribing initially some double-humped distributions, e.g., each hump being of a sech form and the distance between the pulses being of order $2T_0(\kappa)$, for small κ the stable propagation was also observed. This shows that the solutions investigated here can be used for transmission. Moreover, recently there has been much interest in the study of dark solitons (see, e.g., Refs. [18,19]). We have also investigated the propagation of dark solitons in fibers near the ZDP. A presentation of that result is in progress.

In summary, higher-order dispersion may lead to the coupling of fundamental solitons into pairs. By constructing bound states out of fundamental solitons in optical fibers near the ZDP we find nonradiating and quite stable solutions if the humps are well separated. For practical purposes, the separation should be of the order of several picoseconds; then the pulses can propagate over thousands of kilometers without significant changes when damping mechanisms are neglected. In future investigations we shall include dissipative and amplifying mechanisms in order to further improve the applicability, but already now we can state that because of the high efficiency of operation near the ZDP this area is promising and should be further investigated.

This work is supported by the Deutsche Forschungsgemeinschaft. S. K. T. thanks the Humboldt foundation for additional support that made this collaboration possible.

- [1] A. Hasegawa and E. Tappert, *Appl. Phys. Lett.* **23**, 142 (1973).
- [2] L. F. Mollenauer, R. H. Stolen, and J. P. Gordon, *Phys. Rev. Lett.* **45**, 1095 (1980).
- [3] G. I. Stegeman and E. M. Wright, *Opt. Quantum Electron.* **22**, 95 (1990).
- [4] O. E. Martinez, R. L. Fork, and J. P. Gordon, *J. Opt. Soc. Am. B* **2**, 753 (1985).
- [5] F. W. Wise, I. A. Walmsley, and C. L. Tang, *Opt. Lett.* **13**, 129 (1988).
- [6] G. P. Agrawal, *Nonlinear Fiber Optics* (Academic, Orlando, FL, 1989).
- [7] P. K. A. Wai, C. R. Menyuk, H. H. Chen, and Y. C. Lee, *Opt. Lett.* **12**, 628 (1987).
- [8] A. S. Gouveia-Neto, M. E. Faldon, and J. R. Taylor, *Opt. Lett.* **13**, 770 (1988).
- [9] K. J. Blow, N. J. Doran, and E. Commins, *Opt. Commun.* **48**, 181 (1983).
- [10] P. K. A. Wai, C. R. Menyuk, Y. C. Lee, and H. H. Chen, *Opt. Lett.* **11**, 464 (1986).
- [11] P. K. A. Wai, H. H. Chen, and Y. C. Lee, *Phys. Rev. A* **41**, 426 (1990).
- [12] G. R. Boyer and X. F. Carloti, *Opt. Commun.* **60**, 18 (1986).
- [13] G. P. Agrawal and M. J. Potasek, *Phys. Rev. A* **33**, 1765 (1986).
- [14] D. Marcuse, *Appl. Opt.* **19**, 1653 (1980).
- [15] H. H. Kuehl and C. Y. Zhang, *Phys. Fluids B* **2**, 889 (1990).
- [16] M. Hofer, M. H. Ober, F. Haberl, and M. E. Fermann, *IEEE J. Quantum Electron.* **28**, 720 (1992).
- [17] V. K. Mezentsev and S. K. Turitsyn, *Sov. Lightwave Commun.* **1**, 263 (1991).
- [18] D. Krökel, N. J. Halas, G. Giuliani, and D. Grischkowsky, *Phys. Rev. Lett.* **60**, 29 (1988).
- [19] Yu. S. Kivshar, Special Issue, "Dark Solitons in Nonlinear Optics," *IEEE J. Quantum Electron.* **29**, 250 (1993).